32nd URSI GASS, Montreal, 19-26 August 2017

Broadband, Wide angle and Polarization-independent RCS Reduction based on Random Combinatorial Phase Gradient Metasurface

Yaqiang Zhuang* (1), Guangming Wang (1), and Qingfeng Zhang(2)
(1) Air and Missile Defense College, Air Force Engineering University, Xi'an 710051, China,
(2) South University of Science and Technology of China, Shenzhen 518055, China

Abstract

This paper presents a novel random combinatorial phase gradient metasurface (RCPGM) to realize radar cross section (RCS) reduction by dispersing reflection energy. Firstly, both one-dimensional (1D) and two-dimensional (2D) PGM are investigated to validate broadband and high efficiency anomalous reflection. The RCPGM is constructed by random distributed eight kinds of supercells, and each supercell has a special phase gradient direction. Simulation results show that the RCPGM achieves 10 dB RCS reduction from 7.2 GHz to 15.6 GHz for both *x* and *y* polarization. The diffuse characteristic of the metasurface is maintained until the oblique incidence angle up to 45°. This paper provides a novel strategy to design diffuse metasurface.

1. Introduction

Metasurfaces, as the two-dimensional version of metamaterials, also have abilities to fully manipulating propagation behavior of electromagnetic (EM) waves, including phase, amplitude, and polarization on transmission or reflection with subwavelength dimension along wave propagation direction [1]. In addition, the most interesting characteristic of metasurface is that it has phase discontinuity at the interface [2]. Thereby, metasuface attracts more attention and has been widely applied in stealth technology [3], anomalous reflection/refraction [4], polarization conversion [5], etc.

RCS reduction is always a hot topic in stealth technologies, especially with growing demand of stealth platform. Typical RCS method such as shaping and loading radar absorbing materials (RAM) suffer from bulky structure, design complexity and narrow band operation. In recent years, the alternative methods of reducing RCS with thin structure and broadband based on metasurface have been investigated comprehensively [6-10]. In [6], the chessboard-like artificial magnetic conductor (AMC) metasurface is proposed to suppress the backward scattering wave and divide the scattering wave into four main lobes along diagonal direction. Some modified regular configuration such as hexagonal chessboard [7] and triangle-type [8] are proposed to increase the number of reflective lobes, which result in a further reduction of bistatic RCS. However, the chessboard-like configuration metasurfaces suffer from fixed scattering angle and the high bistatic RCS. Then, the random phase metasurfaces are designed to address those disadvantages [9-10]. This phase distribution of metasurface is randomized, which the phase shift of each meta-particle is manipulated by variable sizes or orientation. The goal of random phase metasurfaces is to diffuse the scattering wave into the whole half space. Another strategy for RCS reduction relies on anomalous reflection which called PGM [11]. The PGM will reflect the incident wave to predefine direction. But the drawback of PGM is similar to the one of chessboard metasurface. Nevertheless, to date, few works were reported to achieve diffusion-like scattering by PGM with high performance.

In this paper, we present a novel strategy to achieve broadband, wide-angle and polarization-independent RCS reduction by RCPGM. We combine eight kinds of supercells with randomized distribution to form the metasurface, and the interval among phase gradient directions of each supercell is 45°. Thereby, the reflected wave can be redirected to many directions resulting in a diffusion-like scattering. The simulation results verify the high performance and show that the 10 dB RCS reduction can be obtained from 7.2 GHz to 15.6 GHz with polarization-independent, and the low-scattering characteristic can be maintained until the incident angle up to 45°.

2. Unit cell design

The unit cell is a sandwich like structure: namely top metallic structure, middle F4B substrate with a thickness of 3 mm and a dielectric constant of 2.65, and bottom metallic ground, as shown in Figure 1. The propose unit cell is an achiral rotationally asymmetric structure which is insensitive to the incident polarization. The metallic structure is composed of cross and cross ring (CCR), and two resonance frequencies are designed to be very close to increase the operation bandwidth and the reflection phase range. The optimum dimensions of the unit cell are p=10 mm, a=0.4 mm, w=2.4 mm. We design six unit cells based on same shape with different dimensions whose phase ranges cover 360°. The simulated reflection phase response curves are plotted in Figure 2. It is clearly seen that the curves are almost linear, and they are nearly parallel with the change of l, showing excellent broadband frequency response as required.

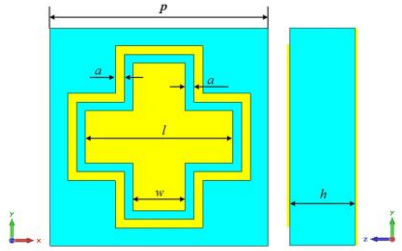

Figure 1. The front view (left) and side view (right) of the unit cell.

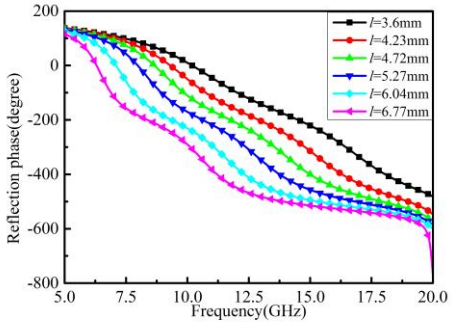

Figure 2. The reflection phase from 5GHz to 20GHz with the change of *l*.

3. Phase Gradient Metasurface Design

As a special kind of metasurface, PGM has been widely used to achieve anomalous reflection. By delicately designing the phase gradients on PGM, the reflected waves can be redirected to desired direction. In this section, we design two kinds of high-efficiency broadband PGM, including 1D PGM and 2D PGM.

3.1 1D phase gradient metasurface

In the 1D case, we design the phase gradient only along *x* direction, as depicted in Figure 3, the red arrow denotes the direction of phase gradient. The reflection angle can be calculated by the Generalized Snell's Law

$$\sin\theta_r - \sin\theta_i = \frac{\lambda_0}{2\pi n_i}\frac{d\Phi}{dx} \tag{1}$$

Where θ_r and θ_i are reflection angle and incidence angle, respectively. λ_0 is the wavelength in free space, and $\frac{d\Phi}{dx}$ denotes the phase gradient. In this design, we utilize six unit cells to realize phase gradient and cover 360° phase range. The phase shift along a single unit cell should be c, where *n* is the number of unit cells. Therefore, the phase gradient can be get as $\frac{d\Phi}{dx}=\frac{\Delta\Phi}{p}=\frac{2\pi}{np}$. Under normal incidence, we get the reflection angle as

$$\theta_r = \arcsin(\frac{\lambda_0}{np}) \tag{2}$$

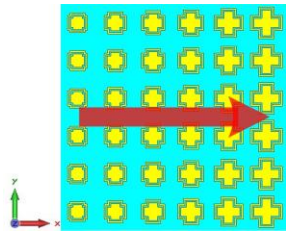

Figure 3. The schematic of the 1D supercell

The supercell of 1D PGM consists of six unit cells with *l*=3.6 mm, 4.23 mm, 4.72 mm, 5.27 mm, 6.04 mm and 6.77 mm can realize a phase shift interval $\Delta\Phi = 60°$ along each unit cell at 10 GHz. To verify the anomalous reflection performance of 1D PGM, a 1D PGM constructed by 4×4 supercells occupies 240mm × 240mm were simulated in CST Microwave Studio. From the near-field and far-field result shown in Figure 4, it is noticeable that the reflected wave was effectively redirected to predefined direction in *xoz* plane.

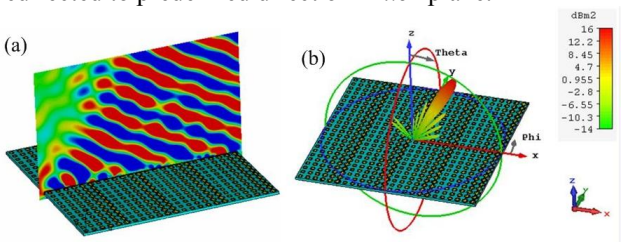

Figure 4. (a)The electric field distribution on *xoz* plane and (b) the 3D far-field scattering pattern at 10 GHz.

3.2 2-D phase gradient metasurface

In the 2D PGM case, the phase gradient along both *x* and *y* direction can lead to out-of-plane anomalous reflection, and the reflected wave can be characterized by two angles: θ_r is the angle between incident and reflected wave and α is the angle between the projection of reflected wave and *x*-axis. As depicted in Figure 5, we distribute six unit cells with different dimensions along *x* and *y* direction respectively, leading to the same phase gradient along both two directions. The red arrow in Figure 5 indicates the direction of synthetic phase gradient.

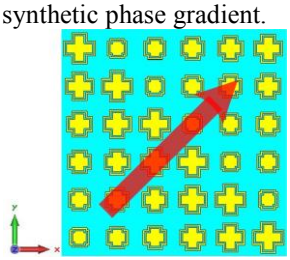

Figure 5. The schematic of the 2D supercell

In terms of 2D case, the Generalized Snell's Law should be modified as

$$\sin\theta_r - \sin\theta_i = \frac{\lambda_0}{2\pi n_i}\sqrt{\left(\frac{d\Phi}{dx}\right)^2+\left(\frac{d\Phi}{dy}\right)^2} \tag{3}$$

As $\frac{d\Phi}{dx}$ is equal to $\frac{d\Phi}{dy}$ in our design, the Eq. (3) is reduced to

$$\sin\theta_r - \sin\theta_i = \frac{\sqrt{2}\lambda_0}{2\pi n_i}\frac{d\Phi}{dx} \quad (4)$$

Under normal incidence, we can calculate θ_r by $\theta_r = \arcsin(\frac{\sqrt{2}\lambda_0}{np})$. The other angle α satisfy $\tan\alpha = \frac{d\Phi}{dy}\Big/\frac{d\Phi}{dx}$ =1, so the α is fixed to 45°. It means that the reflected waves are redirected in diagonal plane.

The numerical simulation of a 240 mm × 240 mm 2D PGM consists of 4 × 4 supercells under normal incidence was carried out in CST Microwave Studio. To give a clear illustration of the out-of-plane anomalous reflection, the electric field distribution on the diagonal plane and 3D far-field scattering pattern at 10GHz are given in Figure 6(a) and (b), respectively. As is expected, an excellent out-of-plane anomalous reflection can realize.

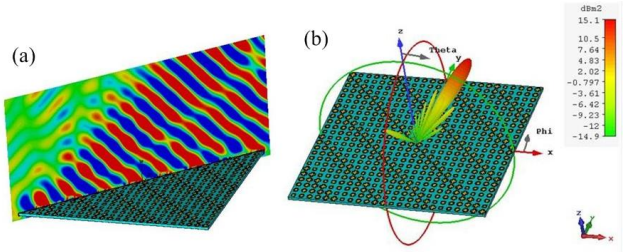

Figure 6. (a)The electric field distribution on diagonal plane and (b) the 3D far-field scattering pattern at 10 GHz.

4. Design of Low-scattering Metasurface and Performance Verification

4.1 Low-scattering Metasurface Design

As demonstrated in above, the 1D and 2D PGM redirect the reflected wave to the desired direction with high efficiency and wideband operation. Then, we design more 1D and 2D supercells by rotating phase gradient direction at the step of 45° in counter anticlockwise direction. As depicted in Figure 7(a) ~ (h), eight kinds of supercells with same amplitude but different direction of phase gradient leading to different reflection angles. If we distribute different kinds of supercell together, the reflection can be regarded as diffusion scattering leading to a radar cross section (RCS) reduction. As shown in Figure 7(i), the RCPGM is designed by distributing 4×4 different supercells randomly. We use the random number generation function to generate 4 × 4 random matrix containing integral numbers from 1 to 16. Each number corresponds to one supercell with specific phase gradient direction. In addition, the supercell signed by 9 ~16 are same to the one signed by 1~8.

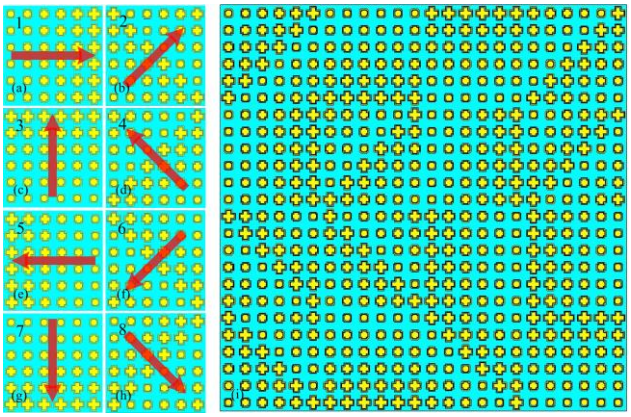

Figure 7. (a~h)The schematic of eight kinds of supercell, (i) the layout of RCPGM

4.2 Simulation and Analysis

We verify the RCS reduction performance of the RCPGM through full wave simulation using CST Microwave Studio. Figure 8 shows the RCS reduction spectrum under normal incidence. The RCS reduction value is calculated by the RCS value of RCPGM minus the one of equal size metallic plate. The 10 dB reduction band is 7.1-15.6 GHz for both *x* and *y* polarization, and the maximum RCS reduction of near 40 dB is obtained at 10.3 GHz. The operation band is broader than the -10 dB mirror reflectivity bandwidth of 1D and 2D PGM, which can be attributed to the interference of different kinds of supercells. To give a clear illustration of RCS reduction, the 3D far-field RCS patterns of RCPGM and metallic plate are given in Figure 9. It is noticeable that the scattering from RCPGM is dispersed into the upper half space at various directions, which obviously differ from the dominating specular reflection for the metallic plate. Therefore, the diffusion scattering results in RCS reduction in the specular direction.

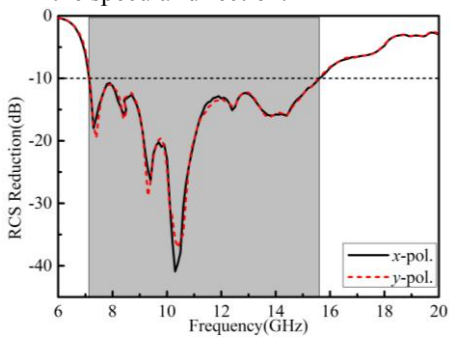

Figure 8. Monostatic RCS reduction under normal incidence

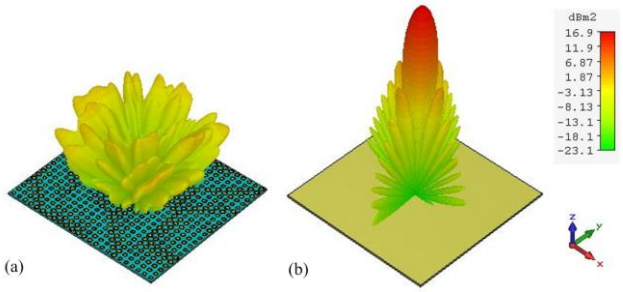

Figure 9. Comparison of 3D RCS pattern of (a) RCPGM and (b) metallic plate under *x*-polarization at 10.3 GHz

Angular performances are investigated to give a comprehensive understanding of RCPGM. The *x* and *y* polarization wave imping from 15°, 30° and 45° in the *xoz* plane are considered. From Figure 10, we can see that the RCS reduction bandwidth decreases a little as the incident angle grows. However, 6 dB RCS reduction bandwidth is still kept broad for both *x* and *y* polarization which means less than 25% power is reflected to backward direction.

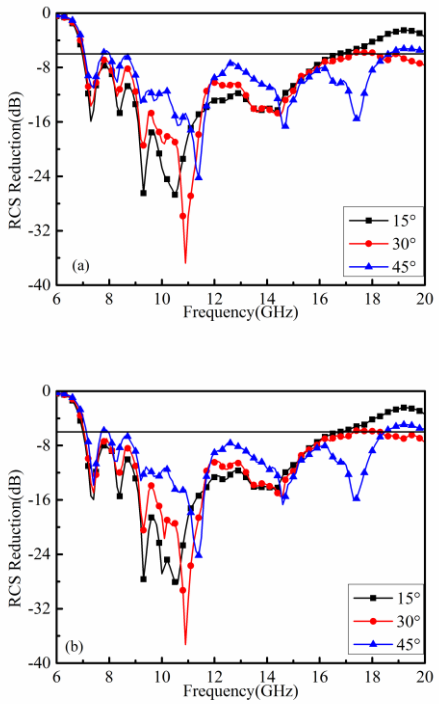

Figure 10. Monostatic RCS reduction under (a) *x*-polarization and (b) *y*-polarization oblique incidence

5. Conclusion

In this paper, a novel strategy for RCS reduction based on metasurface is proposed. The RCPGM consists of eight kinds of supercells can disperse reflected energy into many directions, which results in a diffusion scattering. This design can achieve 10 dB monostatic RCS reduction from 7.2 GHz to 15.6 GHz for both *x* and *y* polarization. The broadband characteristic are well preserved until the oblique incident angle up to 45°. The proposed strategy has been verified by numerical results.

6. Acknowledgements

This work is partially supported by the National Nature Science Foundation of China (61372034, 61401191), Guangdong Natural Science Funds for Distinguished Young Scholar (2015A030306032, S201305014223). Shenzhen Science and Technology Innovation Committee funds (KQJSCX201602 26193445, JCYJ20150331101823678).

7. References

1. L. Zhang, S. Mei, K. Huang, and C. Qiu, "Advances in Full Control of Electromagnetic Waves with Metasurfaces," *Adv. Optical Mater.*, **4**, 6, March 2016, pp. 818–833. doi: 10.1002/adom.201500690.

2. N. Yu, P. Genevet, M. A. Kats, F. Aieta, J.-P. Tetienne, F. Capasso, and Z. Gaburro, "Light Propagation with Phase Discontinuities: Generalized Laws of Reflection and Refraction," *Science*, **334**, 6054, October 2011, pp. 333–337. doi: 10.1126/science.1210713.

3. J. Chen, Q. Cheng, J. Zhao, D. S. Dong, and T. J. Cui, "Reduction of Radar Cross Section Based on a Metasurface," *Prog. Electromagn. Res.*, **146**, April 2014, pp. 71–76. doi: 10.2528/PIER14022606.

4. N. K. Grady, J. E. Heyes, D. R. Chowdhury, Y. Zeng, M. T. Reiten, A. K. Azad, A. J. Taylor, D. A. R. Dalvit, H.-T. Chen, "Terahertz Metamaterials for Linear Polarization Conversion and Anomalous Refraction," *Science*, **340**, 6138, June 2013, pp. 1304–1307. doi: 10.1126/science.1235399.

5. H. Zhu, S. Cheung, K. L. Chung, and T. Yuk. "Linear-to-circular Polarization Conversion Using Metasurface," *IEEE Trans. Antenn. Propag.*, **61**, 9, September 2013, pp. 4615–4623. doi:10.1109/TAP.2013.2267712.

6. M. Paquay, J.C. Iriarte, I. Ederra, R. Gonzalo, and P. de Maagt, "Thin AMC Structure for Radar Cross-Section Reduction," *IEEE Trans. Antennas Propag.* **55**, 12, December 2007, pp. 3630–3638. doi: 10.1109/TAP.200-7.910306.

7. W. G. Chen, C. A. Balanis, and C. R. Birtcher, "Checkerboard EBG Surfaces for Wideband Radar Cross Section Reduction," *IEEE Trans. Antennas Propag.* **63**, 6, June 2015, pp. 2636–2645. doi: 10.1109/TAP.2015.2414-440.

8. T. Hong, H. Dong, J. Wang, H. Ning, Y. Wei, and L. Mao, "A Novel Combinatorial Triangle-type AMC Structure for RCS Reduction," Microwave Opt. Technol. Lett., **57**, 12, December 2015, pp. 2728-2732. doi: 10.1002/mop. 29427

9. X. Yan, L. Liang, J. Yang, W. Liu, X. Ding, D. Xu, Y. Zhang, T. Cui, and J. Yao, "Broadband, Wide-angle, Low-scattering Terahertz Wave by a Flexible 2-bit Coding Metasurface," *Opt. Express*, **23**, 22, November 2015, pp, 29128-29137. doi: 10.1364/OE.23.029128.

10. K. Chen, Y. Feng, Z. Yang, L. Cui, J. Zhao, B. Zhu, and T. Jiang, "Geometric Phase Coded Metasurface: from Polarization Dependent Directive Electromagnetic Wave Scattering to Diffusion-like Scattering," *Sci. Rep.*, **6**, October 2016, p. 35968. doi: 10.1038/srep35968.

11. Y. Li, J. Zhang, S. Qu, J. Wang, H. Chen, Z Xu, and A. Zhang, "Wideband Radar Cross Section Reduction using Two-dimensional Phase Gradient Metasurface," *Appl. Phys. Lett.*, **104**, June 2014, p. 221110. doi: 10.1063/1.4881935.